Stochastic Planning of a Multi-microgrid considering Integration of Renewable Energy Resources and Real-time Electricity Market

Seyed Mehdi Hakimi[a,*], Arezoo Hasankhani[b], Miadreza Shafie-khah[c], João P.S. Catalão[d]

[a]*Electrical Engineering Department and Renewable Energy Research Center, Damavand Branch, Islamic Azad University, Damavand, Iran.*
[b]*College of Engineering and Computer Science, Florida Atlantic University, Boca Raton, FL 33431, USA.*
[c]*School of Technology and Innovations, University of Vaasa, 65200 Vaasa, Finland.*
[d]*Faculty of Engineering of University of Porto, and INESC TEC, Porto, Portugal.*

Abstract

This paper presents a stochastic planning algorithm to plan an operation of a multi-microgrid (MMG) in an electricity market considering the integration of stochastic renewable energy resources (RERs). The proposed planning algorithm investigates the optimal operation of resources (i.e., wind turbine (WT), fuel cell (FC), Electrolyzer, photovoltaic (PV) panel, and microturbine (MT)) and energy storage (ES). Various uncertainties (e.g., the power production of WT, the power production of PV, the departure time of electric vehicle (EV), the arrival time of EV, and the traveled distance of EV) are initially forecasted according to the observed data. The prediction error is estimated by fitting the forecasted data and observed data using a Copula method. A Cournot equilibrium and game theory (GT) are applied to model the real-time electricity market and its interactions with the MMG. The proposed algorithm is examined in a sample MMG to determine the operation of uncertain resources and ES. The obtained results are compared with a baseline and the other conventional optimization methods to verify the effectiveness of the proposed algorithm. The obtained results authenticate the importance of modeling the interaction between the MMG and electricity market,

*Corresponding author at: Electrical Engineering Department and Renewable Energy Research Center, Damavand Branch, Islamic Azad University, Damavand, Iran.

Email addresses: sm_hakimi@damavandiau.ac.ir (Seyed Mehdi Hakimi), ahasankhani2019@fau.edu (Arezoo Hasankhani), mshafiek@univaasa.fi (Miadreza Shafie-khah), catalao@fe.up.pt (João P.S. Catalão)

especially under the high integration of uncertain RERs, resulting in above 8% cost reduction in the MMG.
Keywords: Energy planning, Electricity market, Multi-microgrid, Renewable energy resources (RERs), Uncertainty.

Nomenclature

Abbreviation

DNO Distribution network operator

DR Demand Response

ES Energy storage

EV Electric vehicle

FC Fuel cell

GT Game theory

MCP Market clearing price

MG Microgrid

MMG Multi-microgrid

MT Microturbine

PV Photovoltaic panel

QPSO Quantum particle swarm optimization

RER Renewable energy resource

RMSE Root mean square error

WT Wind turbine

Indices and Sets

i Microgrid

n Microgrid nodes

t Time

y Planning horizon

Parameters

α Cournot factor ($\$/kW^2$)

α^{PV} Temperature factor of PV ($1/^{\circ}C$)

η Efficiency (%)

η_{bat}^{EV} Efficiency of battery of EV (km/kWh)

η_{r}^{PV} Rated efficiency of PV (%)

a_t/d_t Arrival time/ departure time (h)

$B_n^{EV}/B_n^{AC}/B_n^{DW}/B_n^{WM}$ Binary variables for presence of EV/ air conditioner/ dishwasher/ washing machine in demand response program at n

$B_{y,n}^{FC}/B_{y,n}^{ES}/B_{y,n}^{MT}$ Binary variables for replacement of FC/ MT at y and n

$B_n^{WT}/B_n^{FC}/B_n^{EL}/B_n^{PV}/B_n^{ES}/B_n^{MT}$ Binary variables for allocation of WT/ FC/ electrolyzer/ PV/ MT/ ES at n

$C^{CC,WT}/C^{CC,FC}/C^{CC,EL}/C^{CC,PV}/CC^{MT}/C^{CC,ES}$ Capital cost of WT/ FC/ electrolyzer/ PV/ MT/ ES ($\$/kW$)

$C^{Ch,EV}/C^{B,EV}$ Cost of EV charger/ battery ($\$/\$/kWh$)

$C_y^{OM,WT}/C_y^{OM,FC}/C_y^{OM,EL}/C_y^{OM,PV}/C_y^{OM,MT}/C_y^{OM,ES}$ Maintenance and operation cost of WT/ FC/ electrolyzer/ PV/ MT/ ES at y ($\$/kW.year$)

$C_n^{RC,FC}/C_y^{RC,ES}/C_n^{RC,MT}$ Replacement cost of FC/ ES/ MT at y ($\$/kW$)

$C_{t,l}^{loss}$ Penalty cost for loss of energy at t and y ($\$/kW$)

$C_{t,y}^{DR}$ Demand response cost at t and y ($\$/kW$)

Cap_{bat} Capacity of battery of EV (kWh)

d Daily distance travelled by EV (km)

$P^{EV,ref}$ Reference power consumption of EV per daily distance traveled by EV (kW/km)

P_{ch}^{EV}/P_{dch}^{EV} Charge/ discharge power of EV (kW)

P_{c}^{EV} Power consumption of EV (kW)

P_{H}^{FC} Power production of hydrogen in FC (W)

$P_{use,t}^{FC}$ Power consumption of FC at t (W)

P_{r}^{PV} Rated power of PV panel at $G = 1000\,W/m^2$ (W)

P_{i} Power of MG ($\$/kW$)

$P_{min}^{ES,ch}/P_{max}^{ES,ch}$ Minimum/ maximum charge rate of ES (kW/h)

$P_{min}^{ES,dch}/P_{max}^{ES,dch}$ Minimum/ maximum discharge rate of ES (kW/h)

$P_{min}^{ES}/P_{max}^{ES}$ Minimum/ maximum capacity of ES (kW)

$P_{min}^{EV,ch}/P_{max}^{EV,ch}$ Minimum/ maximum charge rate of EV (kW/h)

$P_{min}^{EV,dch}/P_{max}^{EV,dch}$ Minimum/ maximum discharge rate of EV (kW/h)

P_{r}^{WT} Rated power of WT (W)

S_{max}^{T} Maximum capacity of transformer (kW)

SI Solar irradiance (W/m^2)

T_{n}^{PV} Normal temperature of PV panel ($^{\circ}C$)

T_{ref} Reference temperature ($^{\circ}C$)

$v_{ci}/v_{co}/v_{r}$ Cut-in/Cut-out/rated speed of WT (m/s)

V_{min}/V_{max} Minimum/ maximum voltage limit (V)

v_w Wind speed (m/s)

Variables

$ENS_{t,y}$ Loss of energy expectation at t and y (kW)

MCP Market Clearing Price($\$/kW$)

P_t^{FC} Output power of FC at t (W)

P_t^{loss} Power loss at t (W)

P_t^{PV} Output power of PV panel at t (W)

$P_{t,l}^{sell}$ Power sold to amin network at t and y (W)

$P_{t,y}^{buy}$ Power bought from main network at t and y (W)

$P_{t,y}^{WM}/P_{t,y}^{DW}/P_{t,y}^{AC}/P_{t,y}^{EV}$ Demand response power of washing machine/ dishwasher/ air conditioner/ EV at t and y (W)

$S^{WT}/S^{PV}/S^{FC}/S^{EL}/S^{ES}/S^{MT}$ Size of WT/ PV/ FC/ Electrolyzer/ ES/ MT (kW)

$V_{n,t,y}$ Voltage at n, t, and y (V)

1. Introduction

Today, renewable energy resources (RERs) are gaining more attraction in both society and the electricity market, which have become a concrete alternative to increase the environmental and economic benefits. However, different challenges have arisen by applying the RERs in the Microgrids (MGs) due to the high intermittencies in these resources [1]. Modifications in the MG structure and going towards the multi-microgrid (MMG) increase these difficulties [2]. Furthermore, the dynamic nature of the electricity market and the corresponding price elasticity have grown the complexities in defining the optimal operation of the MMG [3]. The main challenge in developing the renewable-based MMG is the increased intermittencies in these resources, which

can be addressed through designing the optimal stochastic energy planning algorithm. Hence, it is crucial to precisely model the uncertainties in the renewable resources and develop an optimal MMG plan.

Various energy planning and management algorithms have been proposed for both MG and MMG to address the optimal operation of these grids. In [4], the optimal size of PV and ES is determined to meet the minimized cost due to the operational constraints. A peak shaving of RERs is investigated through planning the electricity market, tested in Sweden [5]. A day-ahead optimization is proposed to manage the RERs, electric vehicles (EVs), and ES due to weather prediction using a mixed-integer linear programming [6]. Multi-objective optimization is designed to size the RERs in the MG considering reliability, economic, renewable technology, and pollution aspects [7]. A planning algorithm is presented, minimizing the cost due to the environmental objectives in the MGs [8].

There exist two main approaches for MMG energy planning, including deterministic energy planning and stochastic energy planning. Among the deterministic energy planning literature, an energy planning algorithm has been developed for the residential MMG, which has been justified with an Australian residential MMG case study [9]. In another study [10], the energy planning algorithm has been devoted to the EVs integration into the MMG. On the other hand, a large body of the literature is devoted to stochastic energy management. For example, a reinforcement learning-based approach has been proposed to decrease the peak-to-average ratio and maximize the profit gained for the MMG [11]. In [12], the stochastic energy planning has been investigated for the MMG, where the uncertainties in the RERs and demand response (DR) programs have also been considered. A stochastic predictive control has been developed for a two-MG case study due to the coupling constraints, where the robustness of the proposed method has been verified through the statistical analysis [13]. To meet the robustness of the MMG under the high intermittencies, authors have investigated decentralized stochastic energy planning for the MMG [14].

Among these energy planning algorithms, i.e., the deterministic algorithm and stochastic algorithm, we focus on the stochastic energy planning algorithm, which is more feasible in practical applications due to the high intermittencies in the RERs.

The uncertainties in load forecasting by a multi-layer neural network and its impact on the day ahead scheduling have been investigated in [15], where the weather forecasting using an adaptive neuro-fuzzy inference system has also been added to the former article to justify a more complex stochastic planning algorithm [16]. A hierarchical structure has been investigated to minimize the total cost and emission in the MMG due to the uncertainties in the RERs and loads [17]. In a similar study in terms of uncertainty analysis, real-time energy planning in the MMG has been addressed through approximate dynamic programming, where the spatiotemporal uncertainties in wind speed have also been considered [18]. Moreover, the multi-objective energy planning approach has been implemented to realize the minimized cost, reduced emission considering the power quality constraints [19]. None of the abovementioned studies have focused on the electricity market model and its interactions with the MMG, resulting in the imperfect model in terms of the MMG and specifically its financial transactions.

Therefore, it is critical to model the electricity market due to its dynamic nature and price elasticity, which directly impacts the performance of the stochastic energy planning algorithm. However, there exist several models for interpreting the electricity transaction and connection structure between the MMG and electricity market, including modeling the relation between MMG and real-time electricity market [20], proposing a secure structure for connection between MMG and the national wholesale electricity market [21], modeling a peer-t-peer electricity market to justify the transactions between prosumers and consumers [22], etc. Still, a limited number of studies have been focused on modeling the interactions between MMG and the electricity market, with an application to stochastic energy planning. A multi-layer stochastic planning has been proposed for the responsive water pumps, where the dynamic electricity market has been modeled [23]. In [24], the authors have focused on the retailer side of the electricity market, where the energy planning has been solved through the robust optimization method due to the chance constraints of both demand and generation. These two studies have been devoted to the specific case, limiting the generalized model to interpret the interactions between MMG and the electricity market. In [25], the transaction between different electricity market participants, including MG, has been modeled through a hierarchal approach with MG in the lower-level and market operator in the

upper-level. This study lacks a detailed uncertainty analysis, which is critical due to the increased implementation of intermittent resources in the MMG.

Furthermore, the stochastic energy planning algorithm has been investigated from different points of view, where considering the reliability constraints guarantees the optimal operation of this planning algorithm, especially in the MMG structure. The integration of an islanded MG into the electricity market is addressed through a wild goat algorithm [2]. A planning algorithm has been investigated to size the resources and ES due to the reliability constraints and cost minimization [26]. Another study [27] has investigated the MG operation due to the uncertainties and reliability constraints, specifically focused on the impacts of the ES on the reliability index. Furthermore, an optimal and reliable operation of the MMG has been justified through a minimized cost objective function under the high penetration of the RERs [28]. Meeting the reliability constraints in the MMG has been justified through the stochastic planning algorithm, where the stochastic optimization has been reformulated as standard quadratic and linear programming problems [29].

On the other hand, to facilitate the RER-based MMG implementation, DR programs should be entirely developed, where the smart homes can participate in the DR programs and interact with the electricity market. For example, the impacts of the DR program integrated into the energy planning algorithm on reducing the total cost of the MG have been shown in [30]. Furthermore, various strategies for pricing of the electricity market, including real-time pricing and time-of-use pricing, have been tested on the MG, where the advantage of introducing the DR programs has also been proved [31]. In [32], the EVs have been highly integrated into the MG, where the stochastic energy planning and DR programs have been applied to realize the optimal operation. In a similar study [33], the main focus has been devoted to an industrial MG, showing the pros of its participation in the DR programs, where the optimal operation has been determined through stochastic energy planning. Although a large body of literature has been devoted to the DR programs and their impacts on the economic benefits to the smart homes and MGs, a few studies have focused on developing long-term stochastic planning to investigate the effects of the DR programs on developing the RER-based MG and specifically its important role in increasing the interactions between the MMG

Table 1: Taxonomy of the stochastic planning and energy management of a microgrid considering integration of renewable energy resources and electricity market.

	Objective and Methodology					Technology								
Ref.	Algorithm	Planning	DR	M&O	Objectives	PV	WT	EV	ES	FC	Electrolyzer	MT	Uncertainty Analysis	Electricity Market
[2]	Stochastic	Short-term	-	✓	Optimal cost and optimal reliability	✓	✓	-	✓	-	-	✓	-	✓
[12]	Stochastic	Short-term	✓	✓	Optimal cost and optimal Operation	✓	✓	-	✓	-	-	-	-	-
[13]	Stochastic	Short-term	-	-	Optimal cost and optimal Operation	✓	✓	-	✓	-	-	-	-	-
[14]	Robust	Short-term	-	-	Optimal cost and optimal Operation	✓	✓	-	✓	-	-	✓	-	-
[15]	Stochastic	Short-term	-	-	Optimal cost and optimal Operation	✓	✓	✓	✓	-	-	-	-	-
[16]	Stochastic	Short-term	-	-	Optimal cost and optimal Operation	✓	✓	✓	✓	-	-	-	✓	-
[17]	Stochastic	Short-term	-	-	Optimal cost and optimal Operation	✓	✓	-	✓	-	-	✓	-	-
[18]	Stochastic	Short-term	-	-	Optimal cost and optimal Operation	✓	✓	-	✓	-	-	✓	✓	-
[19]	Stochastic	Short-term	✓	-	Optimal cost and optimal Operation	✓	✓	✓	✓	-	-	-	-	-
[23]	Stochastic	Short-term	✓	-	Optimal cost and optimal Operation	✓	✓	-	✓	-	-	-	-	✓
[24]	Stochastic	Short-term	-	-	Maximized risk-sensitive cost	-	-	-	-	-	-	-	-	✓
[25]	Stochastic	Short-term	✓	-	Optimal cost and optimal Operation	✓	-	-	✓	-	-	-	-	✓
[27]	Stochastic	Short-term	✓	-	Optimal cost and optimal reliability	✓	✓	-	✓	✓	-	✓	-	✓
[28]	Stochastic	Short-term	-	-	Optimal cost and optimal operation	-	✓	-	✓	-	-	-	-	-
[29]	Stochastic	Short-term	-	✓	Optimal cost and optimal operation	-	✓	-	✓	-	-	-	-	-
[30]	Stochastic	Short-term	✓	-	Optimal cost and optimal operation	✓	✓	✓	✓	✓	-	✓	-	-
[31]	Stochastic	Short-term	✓	-	Maximized profit and optimal operation	✓	✓	-	✓	-	-	-	-	-
[32]	Stochastic	Short-term	✓	-	Optimal cost and optimal operation	-	✓	✓	✓	-	-	-	-	-
Ours	Stochastic	Long-term	✓	✓	Optimal cost, Optimal Size of RERs, ES, and optimal MCP	✓	✓	✓	✓	✓	✓	✓	✓	✓

and electricity market. Therefore, increasing the MMG interactions with the electricity market can highlight the role of a ”price maker”. Taxonomy of the stochastic planning and energy planning for the RER-based MGs are presented in Table 1.

It should be noted that the MMG has been assumed ”price taker” in the previous studies, where the MGs do not affect the electricity market. However, one of the main goals of developing the MMG is to increase the RERs, where due to integrating the increased RERs into the grid, the RER-based MMG should participate in the electric-

ity market. Hence, the RER-based MMG will interpret as a "price maker" that will affect the electricity market, which is ignored in the previous studies. Using the ES, introducing the DR programs into the MGs, and the reducing cost of the RERs [34] have been investigated as the practical solutions to develop the RER-based MMG. The RER-based MMG is justified to interpret as the price maker in the electricity market, which can operate either independently or as the MG aggregator. Therefore, investigating long-term stochastic planning is essential to determine the optimal size of resources in the MMGs, assuming the MMGs as the price maker.

To the best of our knowledge, until now, there exists no planning algorithm to consider the operational, economic, reliability, and stochastic aspects of an MMG at the same time. Hence, our paper aims to propose the stochastic planning algorithm to address RER-based MMG considering the real-time electricity market. The Cournot equilibrium and GT model are applied to model the real-time electricity market and its interactions with an MMG as a price maker. Therefore, the optimal capacities of RERs (i.e., WT, PV, and FC), non-renewable resources (i.e., MT), electrolyzer, and ES are determined due to the operational constraints. The final goal is to find the minimized cost, where the system constraints and reliability constraints are considered. The high investment cost of RERs is one of the most important challenges in developing these systems in smart MG. This issue can be addressed with optimal sizing of RERs, which simultaneously decreases the total cost of MMG. On the other hand, the output power of RERs, as well as the power consumption of EVs, are forecasted through the observed data, where the Copula method is applied to improve the prediction error.

The contributions of our paper are discussed as follows:

1. A stochastic planning algorithm is presented to determine the optimal operation of an MMG due to the operational constraints and fairly minimize the MGs' costs in an MMG.
2. The GT and Cournot model are applied to model the real-time electricity market and its interactions with an MMG as a price maker.
3. The stochastic planning algorithm accounts for the uncertainties in the RERs and EV, initially forecasted through the observed data and estimated using the

Copula algorithm to improve the prediction error.

4. The stochastic preservation for the EV uncertain variables (arrival time of EV, departure time of EV, and traveled distance) is justified through a detailed uncertainty analysis that investigates the marginal structure and second-order dependence structure.

The rest of this paper is organized as follows: The structure of an MMG is modeled in Section 2. In Section 3, the power models of RERs and EV are presented, where the objective function and its constraints are detailed. Section 4 discusses the uncertainty modeling. The proposed methodology is presented in Section 5. Section 6 elaborates on the case study. The simulation and its obtained results are presented in Section 7. Eventually, the conclusions are expressed in Section 8.

2. Model Structure of Multi-microgrid

A stochastic planning algorithm is presented in this paper to investigate the integration of the uncertain RERS into an MMG and real-time market. A schematic of the MMG structure and its interactions with the real-time market is illustrated in Figure 1, including three MGs, distribution network operator (DNO), and the main network. MG1 is equipped with the WT, PV panel, FC, electrolyzer, and hydrogen tank. Further, MG2 includes the WT, PV panel, and ES. Finally, the WT, PV panel, MT, and ES operate in the MG3. Hence, the proposed MMG model considers the impacts of various resources. The MMG is connected to the DNO, where each MG sends its power bid to the DNO.

Furthermore, the DNO receives the forecasted price from the main network. Hence, the DNO is responsible for managing all power bids and suggested prices. The MMG is connected to the electricity market as a price maker, but the main network's suggested price highly impacts the MCP. It should be noted that the significant role of the main network in the current structure of the electricity network results in high dependency on the main network. However, the increased integration of the MMG reduces the dependency on the main network and can highlight the importance of the MMG as the price maker. It should be noted that the MMG is assessed as the price maker, where it

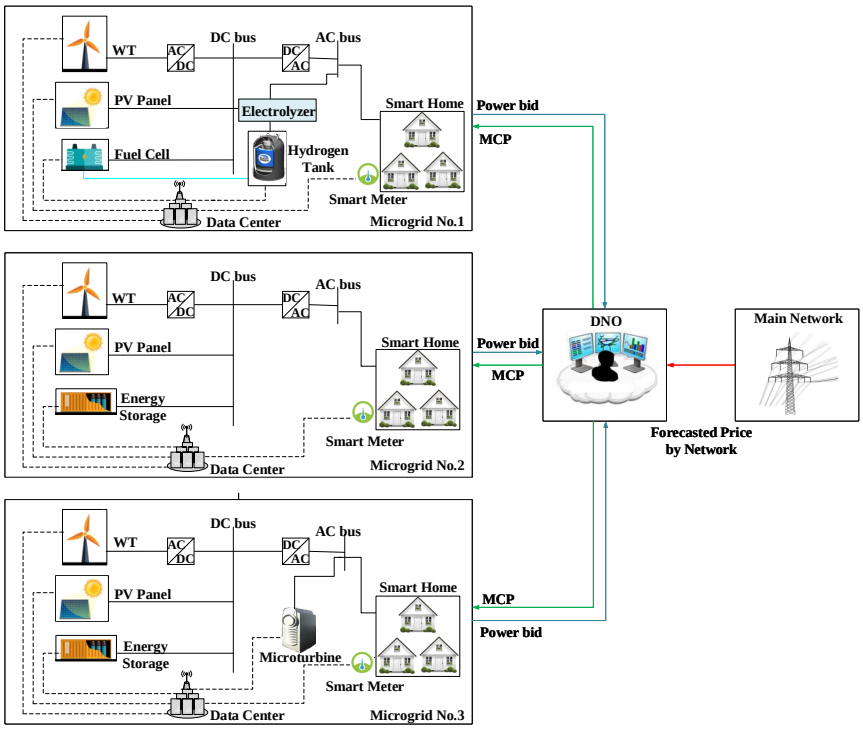

Figure 1: Schematic of a multi-microgrid and its interaction with the real-time electricity market.

interacts with the real-time electricity market to determine the best structure for future MMG.

The MMG should keep a two-way connection with the DNO according to the market structure, where the MMG aims to minimize its total cost. It is crucial to develop the planning algorithm to fairly minimize the cost of all MGs due to their interactions in the MMG structure. Hence, minimizing the total cost of MMG is a complicated problem, which should be precisely solved. The game theory (GT) model is used to determine the interactions between MMG and real-time electricity market [35, 36, 37, 38, 39]. It should be noted that each MG should carefully assess its power and price bids to maximize its profit. Further, each MG can independently propose, and its bids are not affected by the other MGs. However, the MGs need to consider their resources, the corresponding specifications, the electricity market, and the conditions of other MGs to gain the highest profit.

Algorithm 1 Proposed algorithm to calculate primary market clearing price.

1: Initialize smart microgrid, electricity market, and main network data
2: **for** each microgrid **do**
3: Calculate marginal cost of microgrid according to its equipment;
4: Announce the marginal costs of microgrids to DNO
5: **end for**
6: Sort purchasing bids from the highest price to the lowest price and obtain demand curve;
7: Sort selling bids from the lowest price to the highest price and obtain supply curve;
8: Intersect demand curve and supply curve and determine primary market clearing price *MCP*;

The MCP is modeled based on the Cournot model and manage the supply and demand for MMG. The DNO determines the primary MCP according to the suggested price by the main network and MMG. The next MCP is calculated by the Cournot model (1) [40, 41, 42, 43], where this procedure stopped when the stop criteria is met, as presented in (1). The proposed algorithm to calculate the primary MCP is presented in Algorithm 1.

$$MCP^{j} = MCP^{j-1} - \alpha \sum_{i=1}^{n} P_i^j \tag{1}$$

3. Mathematical Modeling

Various RERs, including PV panel, WT, and FC, as well as non-RERs (i.e., MT), are included in the MMG. The mathematical model of each unit is presented in this section, where the power model of the EV is also formulated. Then, the objective function of the stochastic planning of the MMG is presented, which aims to minimize the total cost of the MMG.

3.1. Photovoltaic panel

The PV panel is applied as the RER to convert the solar energy to electricity, where the output power is calculated by (2) [44]. The efficiency of PV η_{PV} is a function of

ambient temperature, as well as the panel temperature, as formulated in (3) [15]:

$$P_t^{PV} = \frac{SI}{1000} \times P_r^{PV} \times \eta^{PV} \tag{2}$$

$$\eta_{PV} = \eta_r^{PV}[1 - \alpha^{PV}(T + SI \times \frac{T_n^{PV} - 20}{800} - T_{ref})] \tag{3}$$

3.2. Wind turbine

The WT is also applied as the RER in this paper, producing the power according to the wind speed and the WT specifications (i.e., cut-in speed, rated speed, cut-out speed). The output power of the WT is formulated as (4) [3].

$$P_t^{WT} = \begin{cases} 0, & v_w < v_{cin} \\ P_r^{WT} \times (\frac{v_w - v_{ci}}{v_r - v_{ci}})^3, & v_{ci} < v_w < v_r \\ P_r^{WT}, & v_r < v_w < v_{co} \\ 0, & v_{co} < v_w \end{cases} \tag{4}$$

3.3. Fuel cell

The FC is included in one of the MGs (i.e., MG1) in an MMG framework, where an integrated WT/PV/FC system operates as the power resources. Although the FC's operation and control have matured substantially over the past years; still the high cost is considered as a barrier to an increased application [45]. However, we will apply the FC in MG1 for the following reasons:

- In this study, since the peak demand occurs in nights, the PV's output power is available over days, applying to produce hydrogen through the electrolysis of water. Hence, the hydrogen production by the RER's power is an apparatus and costly method, which is enabled based on the MG's structure. The FC output power supplies the demand overnight when the PV panel and WT cannot meet the high demand.

- The FC's cost has recently decreased according to its application, showing up to a 60% reduction since 2006 [46]. Therefore, it will be forecasted that this decreasing trend will continue in the future and increase the FC's applications.
- Due to the low accessibility to natural gas for heating applications, the FC is an appropriate option, supplying both electricity and heat. Hence, the FC can supply the hot water to meet the heating of the residential MG1, resulting in a lower dependency on natural gas.
- The FC's dynamic response is fast (i.e., 1 to 3 seconds), which can improve the MG's stability [47].
- Finally, selling the excess produced hydrogen by the FC can benefit the MG1, compensating for the high cost of the FC [48].

The produced power by the FC P_t^{FC} is calculated as follows [49]:

$$P_t^{FC} = P_H^{FC} \times \eta^{FC} - P_{use,t}^{FC} \tag{5}$$

3.4. Electric vehicle

The EV can operate as the controllable loads in the smart homes in the MMG, which can be connected to the network. Hence, the EV can also be considered as the ES, charging through the power injected by the RER. In this regard, the EVs can participate in the DR program as the controllable loads [44, 50], assuming that the EV departs smart home at d_t and arrives smart home at a_t. The power of EV is calculated by (6), while the EV is not available at home over $[d_t, a_t]$ [51]:

$$P_t^{EV} = P_0^{EV} - P_c^{EV} + \sum_t (P_{ch}^{EV} - P_{dch}^{EV}); \quad a_t < t < d_t \tag{6}$$

where, the power consumption of EV is calculated due to the reference power consumption of EV and traveled distance, as follows:

$$P_c^{EV} = P^{EV,ref} \times d \tag{7}$$

Also, the state of charge of EV, which determines the charge power of EV, is formulated by (8) [52]:

$$SoC = 100 \times (1 - \frac{d}{\eta_{bat}^{EV} \times Cap_{bat}}) \tag{8}$$

3.5. Objective function

The objective function is defined to minimize the total cost of MMG considering its participation in the real-time electricity market. Hence, it is important to model the cost of each unit in the MMG (i.e., WT, PV, Electrolyzer, FC, ES, MT), as well as the cost of electricity transactions with the main network (i.e., selling or buying electricity). Further, the cost of participating residential consumers in the DR and the reliability cost should be modeled. It should be notified that the cost of each unit in MG should be precisely modeled.

The objective function of each MG is presented in (9), where the main objective function is formulated as (10). The objective function includes the cost of buying electricity from the main network, the cost of selling electricity to the main network, the cost of the PV, the cost of the WT, the cost of the electrolyzer, the cost of FC, the cost of MT, the cost of participating in the DR program, and the cost of reliability. The decision variables of the objective function are optimal sizes of WT, PV, FC, electrolyzer, ES, MT, and the MCP. Each term of the objective function (9) is precisely modeled in (12)-(22). The cost of buying electricity from the main network is formulated as (12) according to the MCP. Similarly, the cost of selling electricity to the main network is modeled according to the MCP (13). The costs of WT, PV, and electrolyzer are modeled by its capital cost and maintenance and operation cost by (14), (15), (17), respectively. The FC, ES, and MT may need replacement during the planning horizon, so the FC cost is defined by its capital cost, maintenance and operation cost, and replacement cost (16), (18), and (19).

Furthermore, the residential MGs consumers can participate in the DR programs and increase their profit (i.e., decrease the total cost). Hence, several residential appliances are assumed as the controllable loads that can be planned through the stochastic plan [44]. The controllable loads in our paper are washing machine, dishwasher, air conditioner, and EV, where the cost of participating in the DR program is formulated in (21). Finally, the MMG reliability is important, and the planning program should meet the reliability and supply all demand. Hence, the reliability cost is formulated in

(22).

$$\begin{aligned} F_{MG_i} = {} & Cost^{buy} - Cost^{sell} + Cost^{PV} + Cost^{WT} + Cost^{El} \\ & + Cost^{FC} + Cost^{ES} + Cost^{MT} + Cost^{EV} - Cost^{DR} + Cost^{ENS} \end{aligned} \tag{9}$$

$$F = \min_{\overline{u}} \sum_{i=1}^{3} F_{MG_i} \tag{10}$$

Where,

$$\overline{u} \in U; U = [S^{WT}, S^{PV}, S^{FC}, S^{EL}, S^{ES}, S^{MT}, MCP] \tag{11}$$

$$Cost^{buy} = \sum_{y=1}^{y_{max}} \sum_{t=1}^{t_{max}} MCP_{t,y} P_{t,y}^{buy} \tag{12}$$

$$Cost^{sell} = \sum_{y=1}^{y_{max}} \sum_{t=1}^{t_{max}} MCP_{t,y} P_{t,y}^{sell} \tag{13}$$

$$Cost^{WT} = \sum_{n=1}^{n_{max}} B_n^{WT} S^{WT} C^{CC,WT} + \sum_{y=1}^{y_{max}} \sum_{n=1}^{n_{max}} B_n^{WT} S^{WT} C_y^{OM,WT} \tag{14}$$

$$Cost^{PV} = \sum_{n=1}^{n_{max}} B_n^{PV} S^{PV} C^{CC\&I,PV} + \sum_{y=1}^{y_{max}} \sum_{n=1}^{n_{max}} B_n^{PV} S^{PV} C_y^{OM,PV} \tag{15}$$

$$\begin{aligned} Cost^{FC} = {} & \sum_{n=1}^{n_{max}} B_n^{FC} S^{FC} C^{CC,FC} + \sum_{y=1}^{y_{max}} \sum_{n=1}^{n_{max}} B_n^{FC} S^{FC} C_y^{OM,FC} \\ & + \sum_{y=1}^{y_{max}} \sum_{n=1}^{n_{max}} B_{y,n}^{FC} S^{FC} C_y^{RC,FC} \end{aligned} \tag{16}$$

$$Cost^{EL} = \sum_{n=1}^{n_{max}} B_n^{EL} S^{EL} C^{CC,EL} + \sum_{y=1}^{y_{max}} \sum_{n=1}^{n_{max}} B_n^{EL} S^{EL} C_y^{OM,EL} \tag{17}$$

$$\begin{aligned} Cost^{ES} = {} & \sum_{n=1}^{n_{max}} B_n^{ES} S^{ES} C^{CC,ES} + \sum_{y=1}^{y_{max}} \sum_{n=1}^{n_{max}} B_n^{ES} S^{ES} C_y^{OM,ES} \\ & + \sum_{y=1}^{y_{max}} \sum_{n=1}^{n_{max}} B_{y,n}^{ES} S^{ES} C_y^{RC,ES} \end{aligned} \tag{18}$$

$$Cost^{MT} = \sum_{n=1}^{n_{max}} B_n^{MT} S^{MT} C^{CC,MT} + \sum_{y=1}^{y_{max}} \sum_{n=1}^{n_{max}} B_n^{MT} S^{MT} C_y^{OM,MT} + \sum_{y=1}^{y_{max}} \sum_{n=1}^{n_{max}} B_{y,n}^{MT} S^{MT} C_y^{RC,MT} \tag{19}$$

$$Cost^{EV} = \sum_{n=1}^{n_{max}} B_n^{EV} (C^{Ch,EV} + C^{B,EV}) \tag{20}$$

$$Cost^{DR} = \sum_{y=1}^{y_{max}} \sum_{t=1}^{t_{max}} \sum_{n=1}^{n_{max}} B_n^{WM} P_{t,y}^{WM} C_{t,y}^{DR} + \sum_{y=1}^{y_{max}} \sum_{t=1}^{t_{max}} \sum_{n=1}^{n_{max}} B_n^{DW} P_{t,y}^{DW} C_{t,y}^{DR} + \sum_{y=1}^{y_{max}} \sum_{t=1}^{t_{max}} \sum_{n=1}^{n_{max}} B_n^{AC} P_{t,y}^{AC} C_{t,y}^{DR} + \sum_{y=1}^{y_{max}} \sum_{t=1}^{t_{max}} \sum_{n=1}^{n_{max}} B_n^{EV} P_{t,y}^{EV} C_{t,y}^{DR} \tag{21}$$

$$Cost^{ENS} = \sum_{y=1}^{y_{max}} \sum_{t=1}^{t_{max}} ENS_{t,y} C_{t,y}^{loss} \tag{22}$$

The constraints of the objective function are modeled as follows. The power equilibrium is modeled in (23), where the sum of all power should meet the demand. The voltage of each bus of the MMG should stay within the acceptable range (24). Moreover, the power transactions should meet the limits of the transformer, as formulated in (25). It should be noted that the power of the PV, WT, FC, MT, and ES should remain within the allowable range determined according to the units' specifications (26)-(35).

$$P_{t,y}^{buy} - P_{t,y}^{sell} - P_t^{loss} + P_{n,t,y}^{WT} + P_{n,t,y}^{PV} + P_{n,t,y}^{FC} + P_{n,t,y}^{MT} \pm P_{n,t,y}^{ES} = P_{n,y}^{D} \tag{23}$$

$$V_{min} \leq V_{n,t,y} \leq V_{max} \tag{24}$$

$$0 \leq P_{t,y}^{buy}, P_{t,y}^{sell} \leq S_{max}^{T} \tag{25}$$

$$0 \leq P_{t,y}^{PV} \leq P_{max}^{PV} \tag{26}$$

$$0 \leq P_{t,y}^{WT} \leq P_{max}^{WT} \tag{27}$$

$$0 \leq P_{t,y}^{FC} \leq P_{max}^{FC} \tag{28}$$

$$0 \leq P_{t,y}^{MT} \leq P_{max}^{MT} \tag{29}$$

$$P_{min}^{ES} \leq P_{t,y}^{ES} \leq P_{max}^{ES} \tag{30}$$

$$P_{min}^{ES,ch} \leq P_{t}^{ES,ch} \leq P_{max}^{ES,ch} \tag{31}$$

$$P_{min}^{ES,dch} \leq P_{t}^{ES,dch} \leq P_{max}^{ES,dch} \tag{32}$$

$$P_{min}^{EV,ch} \leq P_{t}^{EV,ch} \leq P_{max}^{EV,ch} \tag{33}$$

$$P_{min}^{EV,dch} \leq P_{t}^{EV,dch} \leq P_{max}^{EV,dch} \tag{34}$$

$$P_{min}^{EV} \leq SOC_{t}^{EV} \leq SOC_{max}^{EV} \tag{35}$$

4. Uncertainty Modeling

In this study, we assume five uncertain variables, including wind speed v_w, solar irradiance SI, arrival time of EV a_t, departure time of EV d_t, and daily distance of EV d. To forecast the uncertain variables used in the stochastic planning algorithm, these parameters are initially modeled according to the historical recorded (i.e., observed) data.

4.1. Modeling of uncertain variables

Solar irradiance and wind speed: To address the uncertainties in the solar irradiance and wind speed, we use the hourly measured data over 5 years at a residential site located in Tehran, Iran (latitude 35.7109 $^{\circ}N$, longitude 51.3114 $^{\circ}E$, and elevation above sea level 1191 m; data from [53]). The mean and standard deviation of the wind speed are 6.37 m/s and 4.27 m/s, respectively. Also, The mean of the solar irradiance is 227.5 W/m^2.

To model the uncertainties in the observed data X, we use the machine learning toolbox in MATLAB, where several methods are tested, and the obtained data (i.e., predicted data) X^* are justified through the mean square error (MSE) and root mean square error (RMSE), formulated as follows.

$$MSE = \frac{1}{n}\sum_{i=1}^{n}(X_i^* - X_i)^2 \tag{36}$$

$$RMSE = \sqrt{\frac{1}{n}\sum_{i=1}^{n}(X_i^* - X_i)^2} \tag{37}$$

To model the uncertainties in the wind speed, normal distribution, Weibull distribution, Gaussian process modeling, and spline method are tested. After fitting different methods, the MSE and RMSE of normal distribution, Weibull distribution, Gaussian process modeling, and spline method are calculated 106.9266 (10.3405 m/s), 43.1965 (6.5724 m/s), 28.3524 (5.3247 m/s), and 14.6751 (3.8308 m/s), respectively, where inside parentheses are the values of the RMSE. The obtained results verify that the spline method shows better performance in modeling the wind speed uncertainties. Furthermore, the solar irradiance observed data are fitted through normal distribution, beta distribution, Gaussian process modeling, and spline method. After testing various methods, the calculated MSE and RMSE for normal distribution, beta distribution, Gaussian process modeling, and spline method are 17.9429 (4.2359 W/m^2), 2.7231 (1.6502 W/m^2), 1.5637 (1.2505 W/m^2), and 0.2234 (0.4726 W/m^2), respectively, where inside parentheses are the values of the RMSE. Hence, the spline method shows the best performance, which is chosen to model both solar irradiance and wind speed.

The spline method consists of flexible functions, as normally interpreted by the piecewise polynomials joined together with a certain degree of smoothness [54]. Among the spline methods, the B-spline of order $k \geq 1$ has gained attention due to its property to be formulated as $X = B\beta + \varepsilon$, where $X \in \{v_w, SI\}$, ε is a sequence of independent and identically distributed random variables with zero mean and finite variance, B is a matrix with B_j defined as follows:

$$B_j^k(x) = \frac{x - t_j}{t_{j+k} - t_j} B_j^{k-1}(x) + \frac{t_{j+k} - x}{t_{j+k} - t_{j+1}} B_{j+k}^{k-1}(x) \tag{38}$$

where, $j \in \{-k, -k+1, ..., k\}$, and t_j denotes as knots and sets the shape of the function selected by the user. To model the uncertain variable X, an estimate of β should be formulated, which is obtained through the least squares criterion and minimizing the residual sum of squares as follows:

$$\widehat{\beta} = (B^T B)^{-1} B^T X \tag{39}$$

Electric vehicle: The uncertainties in EV are commonly interpreted with three variables, including arrival time a_t, departure time d_t, and travelled distance d. To model these uncertain variables, three probability distribution functions (PDFs) presented in [55] are used, as follows:

$$f(a_t) = \frac{1}{\sigma_a}(1 + k_a(\frac{t - \mu_a}{\sigma_a}))^{-(1+\frac{1}{k_a})} e^{-(1+k_a(\frac{t-\mu_a}{\sigma_a}))^{-\frac{1}{k_a}}} \tag{40}$$

$$f(d) = \frac{1}{\sigma_d}(1 + k_d(\frac{d - \mu_d}{\sigma_d}))^{-(1+\frac{1}{k_d})} e^{-(1+k_d(\frac{d-\mu_d}{\sigma_d}))^{-\frac{1}{k_d}}} \tag{41}$$

$$f(d_t) = \frac{\beta}{\alpha}(\frac{t}{\alpha})^{(\beta-1)} e^{-(\frac{t}{\alpha})^{\beta}} \tag{42}$$

It should be noted that the estimated uncertain variables correspond with error, which can be decreased through improving the prediction precision. In this paper, we apply the Copula algorithm according to the presented method in [56], where the Copula algorithm has been used to decrease the prediction error and improve the estimation. Hence, the Copula algorithm and the proposed method to improve the prediction are discussed in the following section.

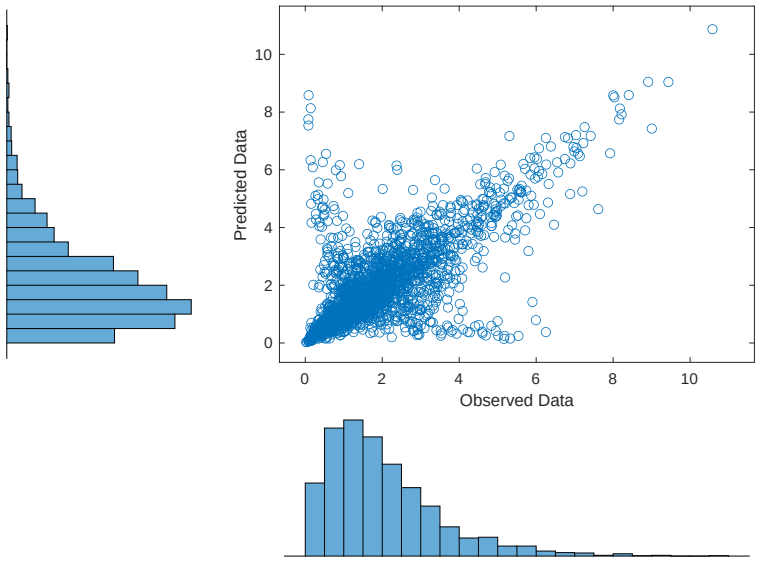

Figure 2: Scatter plot of the observed data along with a predicted data.

4.2. Copula-based algorithm for uncertainty modeling

As discussed, the Copula algorithm is applied to improve the prediction error, which has been initially proposed in [56]. Hence, the predicted data of uncertain variables are justified with the observed data over the same period, where the joint conditional distribution estimation of prediction error is generated through the Copula algorithm (Figure 2). As illustrated in Figure 2, a sample time series of the observed data is compared with the predicted data to highlight the difference between these two data and the importance of applying the Copula algorithm. Note that Figure 2 is only an illustration for sample data, and detailed uncertainty analysis on the stochastic variables of our paper (solar irradiance, wind speed, arrival time of EV, departure time of EV, and traveled distance of EV) are presented in Section 7.2.1. Let $\widehat{X}$ represents the estimation from the uncertain variable of X, and X^* denotes the predicted variable, where the estimation is improved through the prediction error e obtained by the Copula algorithm formulated as follows:

$$\widehat{X} = X^* + e \tag{43}$$

To obtain the prediction error e, the joint conditional distribution should be calculated through the Copula function C. Assuming that $F_X(x) = u$ and $F_{X^*}(x^*) = v$, the joint distribution between observed uncertain variable X and predicted X^* is determined as follows:

$$F_{XX^*}(x, x^*) = C(F_X(x), F_{X^*}(x^*)) \tag{44}$$

where, the joint conditional distribution is obtained as follows:

$$C(u, v) = F(x, x^*) = F(F_X^{-1}(u), F_{X^*}^{-1}(v)) \tag{45}$$

To construct the Copula function, an Archimedean method is used, which is thoroughly discussed in [57] and briefly explained here, as well as the basic specifications of the Copula function.

Copula function: Copula functions C are defined as functions to couple multivariate distribution functions and showing as a one-dimensional marginal distribution function [58], where C includes n variables $X \in [0,1]^n$. The main specifications of the Copula functions are: (i) $C \in [0,1]$; (ii) $C(u)$ is zero if at least one coordinate u_i is zero, assuming $u = [u_1, ...u_n] \in [0,1]^n$; and (iii) $C(u) = u_i$ if all coordinates are one except u_i. In this study, among Copula functions, such as Gaussian Copula and Archimedean Copula, we choose an Archimedean method to obtain the Copula functions. The Archimedean Copula is selected since it has a closed form, which is suitable to interpret various dependence structures; still, the Archimedean Copula is not derived from multivariate distributions by Sklar's theorem, resulting in some doubts in its efficiency in higher-dimension Copulas [59]. Therefore, Copula function $C(u)$ is obtained by the Archimedean method as follows [60]:

$$C(u|\alpha) = \phi^{-1}(\sum_{i=1}^{n} \phi(u_i)) \tag{46}$$

where, α is the parameter of the Archimedean Copula, and $\phi(.)$ is a generator function defined by (47) for Frank Archimedean Copula:

$$\phi = -log(\frac{exp(-\alpha u) - 1}{exp(-\alpha) - 1}) \tag{47}$$

In our problem, the Copula is applied to find the joint distribution between observed uncertain variable and predicted variables so that $n = 2$ in (46), which is rewritten as

follows [59]:

$$C(u,v) = \frac{-1}{\alpha} log(1 + \frac{(exp(-\alpha u) - 1)(exp(-\alpha v) - 1) - 1}{exp(-\alpha) - 1}) \tag{48}$$

4.3. Uncertainty analysis

To investigate the uncertainties of the stochastic variables, an uncertainty analysis is performed in this paper. In this regard, the marginal structures of the stochastic variables are modeled through the L moment, which can also be addressed through the central moments [61]. Furthermore, the dependence structures of the stochastic variables are analyzed through an index named climacogram (i.e., variance of the averaged stochastic variable $\overline{x}^{(k)}$ vs. continuous time scale in time units k) [61]. It should be noted that the climacogram is linked to the autocovariance; still, climacogram shows less bias compared to the autocovariance [62].

5. Proposed Methodology

The main objective of our stochastic planning algorithm is to determine the optimal operation of the MMG, where the RERs and ES are optimally sized. There exist several motivations and drivers behind our proposed methodology to address the stochastic energy planning of the MMG. First, the MMG is assumed "price maker" despite the previous studies, where the MMG has been considered a "price taker". Since the environmental concerns motivate the increased RERs, the RER-based MMG will highly penetrate in the near future, and it is of interest to evaluate the MMGs as the price makers and investigate their interactions with the electricity market. Second, the RER-based MMG has become a feasible and practical option through using the ES and DR programs, which are investigated in our paper to balance the size of RERs, stability, and MMG's costs. Third, the demand side should participate in the power transactions to address the environmental issues, energy crisis, increased RERs, and reliability that are thoroughly investigated in our paper. Finally, it is critical to devise long-term stochastic planning for the MMG to manage its operation due to the uncertain parameters. We present long-term stochastic energy planning of the MMG considering the increased

Algorithm 2 Algorithm to manage multi-microgrid considering its participation in a real-time electricity market.

Initialize wind speed, solar irradiance, loads, and features of resources and energy storage in multi-microgrid;
for $i = 1, ..., N_i$ **do**
    for each microgrid **do**
        Optimize each microgrid according to its objective function;
        Announce power bid from each microgrid to distribution network operator;
    end for
    Check the constraints of objective function (23)-(35);
    Calculate Market Clearing Price MCP and announce it to microgrids;
    Check Cournot equilibrium $\Delta MCP = MCP^{i} - MCP^{i-1}$;
    if $\Delta MCP = 0$ **then**
        Obtain optimal size of resources and energy storage in the multi-microgrid;
    else
        $i = i + 1$
    end if
end for

integration of the uncertain RERs and the existence of a two-way interaction between MMG and the electricity market.

The stochastic planning algorithm is presented in Algorithm 2, where the MMG interacts with the real-time electricity market. In our proposed algorithm, each MG should be optimized in the MMG framework so that the optimal operation is satisfied for all MGs, interacting with the real-time electricity market and operate as the price maker. The RESs and ES are optimally sized when the Cournot equilibrium is met, and the final MCP is determined.

A detailed flowchart of our proposed stochastic planning algorithm is demonstrated in Figure 3. As shown in this figure, the stochastic planning algorithm is initialized by the environmental, load, MG, and EV data, where the technical specifications of resources and ES should also be defined as the inputs for the algorithm. The future

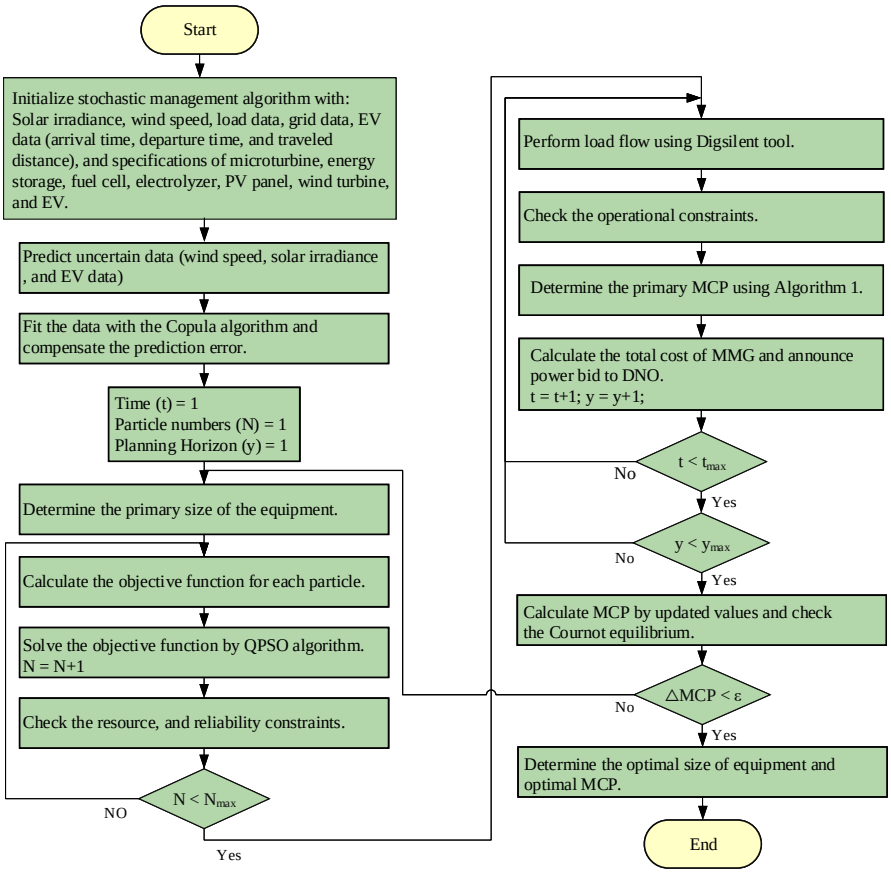

Figure 3: Flowchart of the proposed stochastic planning algorithm to determine the optimal operation of the multi-microgrid under its interaction with the real-time electricity market.

wind speed, solar irradiance, arrival time of EV, departure time of EV, and traveled distance of EV are forecasted using the smoothing spline method discussed in Section 4. The predicted data and the true data are fitted through the Copula algorithm to reduce the prediction error, where the prediction error is modeled. Hence, the predicted data are revised according to the prediction error, and more precise estimation is achieved.

After setting time, particle number, and planning horizon to 1, the size of the resources and ES are determined by the initial guesses. For each particle, the objective function (10) is solved through the QPSO algorithm due to the predefined constraints (23)-(35). Then, the load flow is performed by the Digsilent tool due to the operational

Algorithm 3 Algorithm to solve optimization problem using QPSO

Initialize parameters of QPSO algorithm;
for $N = 1, 2, ..., N_{iteration}$ **do**
    for each decision variable **do**
        calculate cost of particle $x_{it}(N)$ using objective function (10);
    end for
    if $Cost(x_{it}(N)) < Cost(P_{bestit})$ **then**
        Put $P_{bestit} = x_{it}$;
    else
        if $Cost(x_{it}(N)) < Cost(G_{bestit})$ **then**
            Put $G_{bestit} = x_{it}$;
        end if
    end if
    Obtain optimal response;
end for

constraints. The primary MCP is determined by Algorithm 1, where the total cost of MMG is calculated and announced to the DNO. The MCP is updated, and the optimal size of the resources and ES are determined when $\Delta MCP < \varepsilon$.

The Algorithm for finding the optimal decision variables using the Quantum Particle Swarm Optimization (QPSO) method is presented in Algorithm 3. As presented in Algorithm 3, the particle cost should be calculated for each decision variable according to the objective function (10). The obtained cost is compared to the best value of that iteration and the best global value. As the QPSO algorithm progresses, it is converged and finds a global minimum very quickly.

5.1. Proposed simulation structure

The schematic of the proposed simulation algorithm is shown in Figure 4. As observed in Figure 4 (a), the main blocks of the simulation algorithm include MMG and QPSO algorithm. The MMG is initialized by the input data, where the objective function is calculated. The QPSO algorithm is applied to minimize the total cost and

find the optimal decision variables (11). The detailed steps of the proposed stochastic planning simulation algorithm are illustrated in Figure 4 (b). The solar irradiance, wind speed, and EV data are considered as the inputs to the prediction block, where the Copula method is applied to improve the prediction error. The objective function is calculated and minimized according to the technical specifications of MGs, loads, resources, and ES, which is minimized by the QPSO algorithm. Finally, the optimal cost, the optimal size of resources and ES, and MCP are found as the outputs of the stochastic planning algorithm.

6. Case Study

In this section, a sample case study is modeled as the MMG, which is used to test the efficiency of our proposed method. A residential MMG is modeled as a case study in our paper, where the detailed line data is presented in [63]. The residential complex named Ekbatan town includes 15500 apartments in an area of 2208570 m^2, located in Tehran, Iran. This residential MMG has three independent sets of buildings called block 1, block 2, and block 3, determined as MGs in our study. The residential MGs are connected to the medium voltage (i.e., 20 kV). A schematic of the case study is shown in Figure 5.

The smart MG1 is equipped with the WT, PV panel, FC, electrolyzer, hydrogen tank, controllable loads (i.e., washing machine, dishwasher, air conditioner, and EVs), and non-controllable loads. The equipment in MG2 is WT, PV panel, ES, controllable loads, and non-controllable loads similar to the MG1. Furthermore, the MG3 includes WT, PV panel, MT, ES, controllable loads, and non-controllable loads, where the controllable loads are washing machine, dishwasher, air conditioner, and EVs. A schematic of nodes of each MG is shown in Figure 5, where the peak demand of each node is shown in Table 2 [64]. It should be noted that the nodes of MG1, MG2, and MG3 are denoted by A_i, B_i, and C_i, respectively. The demand profile of the modeled residential MMG is shown in Figure 6, based on the real measured peak demand data given from the Iran grid planning company [64] and the normalized IEEE residential load curve [65]. The normalized load curve (Figure 6 (a)) is the basis to calculate the

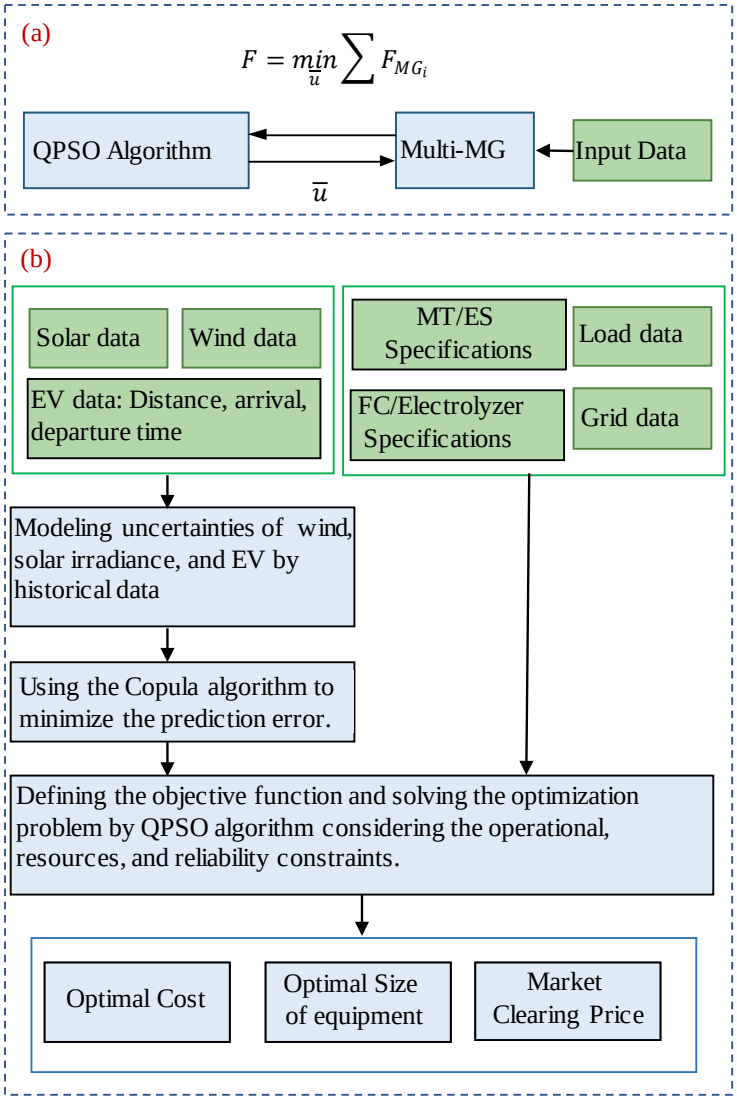

Figure 4: Schematic of the proposed simulation algorithm: (a) main blocks of the simulation algorithm; (b) detailed steps of the proposed stochastic planning simulation algorithm.

demand for each node of the MMG, where a sample annual load profile of node A1 is shown in Figure 6 (b).

It should be noted that we assume an hourly representation for the load in our paper to address long-term planning and stochastic planning for the MMG, which have been

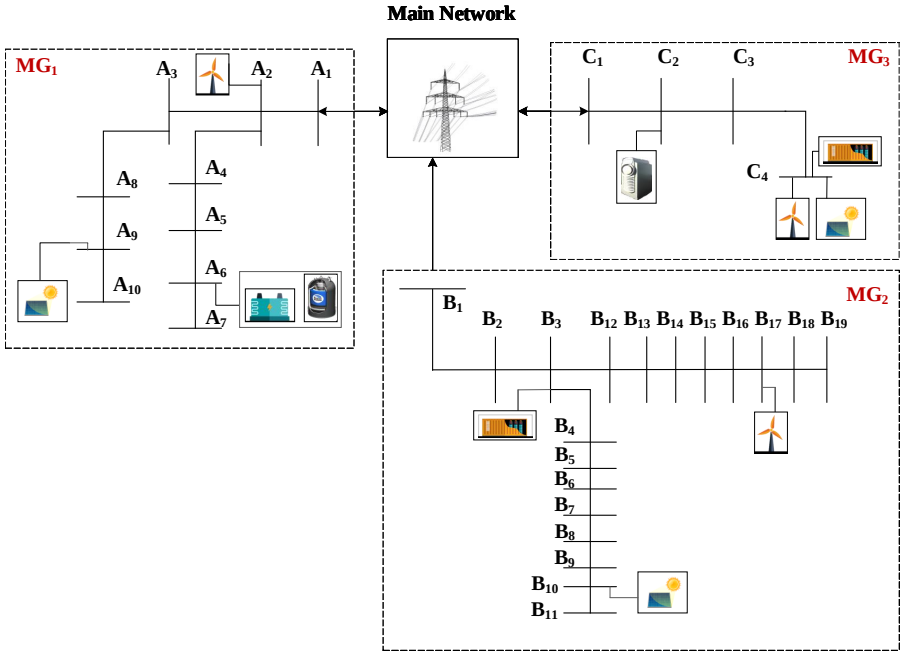

Figure 5: Schematic of case study, including three microgrids.

Table 2: Peak demand of each node for the residential multi-microgrid.

Node	A_1	A_2	A_3	A_4	A_5	A_6	A_7	A_8	A_9	A_{10}	B_1
Peak Demand $[kW]$	500	500	500	500	500	600	600	600	600	500	300
Node	B_2	B_3	B_4	B_5	B_6	B_7	B_8	B_9	B_{10}	B_{11}	B_{12}
Peak Demand $[kW]$	400	400	500	500	400	500	500	400	400	400	400
Node	B_{13}	B_{14}	B_{15}	B_{16}	B_{17}	B_{18}	B_{19}	C_1	C_2	C_3	C_4
Peak Demand $[kW]$	500	500	300	300	300	600	300	600	600	400	400

verified as an adequate option for the long-term planning and management in the MGs [2, 23, 66]. Hence, all input data are represented on an hourly basis. Further, a large number of parameters are included in this paper, which will increase the complexity of the problem. On the other hand, since the MMG is planned to interact with the electricity market, the clearing time is also an essential factor in defining the timestep basis in our study. Therefore, we choose the hourly basis for our study to justify the

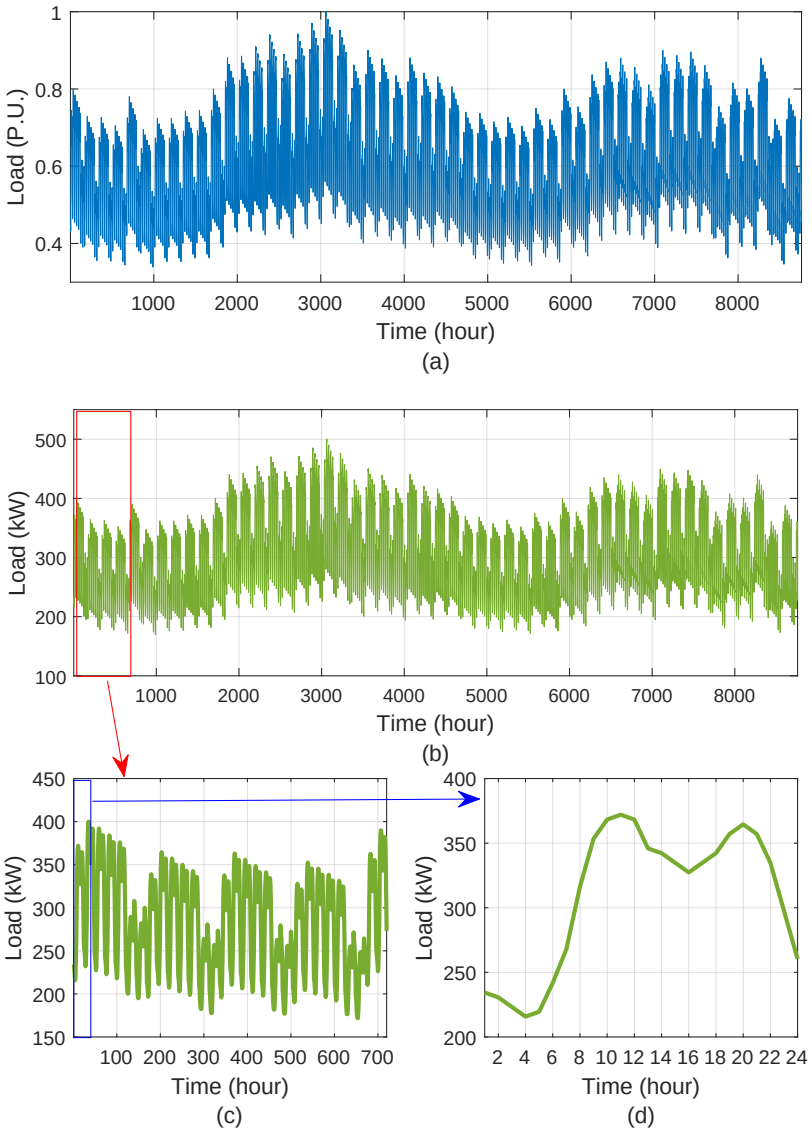

Figure 6: Load profile: (a) normalized load profile of the multi-microgrid; (b) annual load profile of node A1; (c) monthly load profile of node A1; (d) daily load profile of node A1.

real electricity market in Iran [67] so that the MCPs are calculated on an hourly basis.

7. Simulation and Results Discussion

In this section, the comparative results of testing our proposed methodology on a sample case study are presented. The proposed stochastic energy planning algorithm is

Table 3: Parameters of wind turbine [69].

Parameters	Value	Unit
$C^{CC,WT}$	1500	$[\$/kW]$
$C^{OM,WT}$	15	$[\$/kW.year]$
v_{ci}	3.5	$[m/s]$
v_r	10	$[m/s]$
v_{co}	25	$[m/s]$
P_r^{WT}	50	$[kW]$

Table 4: Parameters of photovoltaic panel [3, 68].

Parameters	Value	Unit
$C^{CC\&I,PV}$	5402	$[\$/kW]$
$C^{OM,PV}$	20	$[\$/kW.year]$
η_{PV}	37	$[\%]$
P_r^{PV}	1	$[kW]$

designed to find the optimal operation of the MMG, where the optimal size of various equipment is found.

7.1. Simulation setup

To show the performance of the proposed method, it is tested on the sample case study presented in Section 6. The MMG is equipped with WT, PV panel, FC, hydrogen tank, and ES. The parameters of the equipment are presented in Table 3 to Table 6. Furthermore, the parameters of EV is presented in Table 7. Note that the EV charger and battery cost are 24000 \$ and 720 $\$/kWh$ [68]. The historical data for the wind speed, solar irradiance, arrival time of EV, departure time of EV, and traveled distance of EV are modeled according to the discussed model in Section 4. Then, the Copula algorithm is used to minimize the prediction errors. The stochastic planning algorithm is applied according to the predicted data and the parameters of all equipment.

Table 5: Parameters of fuel cell and electrolyzer [70].

Parameters	Value	Unit
$C^{CC,FC}$	3000	$[\$/kW]$
$C^{OM,FC}$	175	$[\$/kW.year]$
$C^{RC,FC}$	2500	$[\$/kW]$
$C^{CC,EL}$	2000	$[\$/kW]$
$C^{OM,EL}$	25	$[\$/kW.year]$

Table 6: Parameters of energy storage [44].

Parameters	Value	Unit
$C^{CC,ES}$	500	$[\$/kW]$
$C^{OM,ES}$	400	$[\$/kW.year]$
$C^{RC,ES}$	400	$[\$/kW]$

7.2. Results

7.2.1. Uncertainty Analysis

In this section, we present the uncertainty analysis of the stochastic variables (i.e., wind speed, solar irradiance, the arrival time of EV, departure time of EV, and distance in our study). To enable this uncertainty analysis, as explained in Section 4, we use the hourly recorded time series of stochastic variables. Also, we compare the observed data along with the estimated data obtained through fitting the appropriate model and the Copula algorithm. To justify an acceptable estimation from a stochastic variable, its marginal structure and second-order dependence structure should be preserved so that we compare these structures for observed data and simulated data (i.e., estimated data). The marginal structure of the stochastic variable can be investigated through the probability distribution function or the first few central or L moments, and we present our results based on the L moments in this paper. Hence, the L moments of the observed data, along with the simulated data for stochastic variables, including wind speed, solar irradiance, the arrival time of EV, departure time of EV, and distance, are presented in Table 8.

As shown in Table 8, the marginal structure is preserved by an error between $\pm 5\%$

Table 7: Parameters of electric vehicle [71].

Parameters	Value	Unit
σ_a	0.85	[*hour*]
μ_a	17.27	[*hour*]
k_a	-0.06	[*hour*]
σ_d	7.12	[*km*]
μ_d	17.66	[*km*]
k_d	0.05	[*km*]
β	21.38	[*hour*]
α	7.67	[*hour*]

Table 8: L moments of the observed data along with the simulated data for stochastic variables, including wind speed, solar irradiance, arrival time of EV, departure time of EV, and distance.

L moment	Wind Speed		Solar Irradiance		Arrival Time		Departure Time		Distance	
	Obs.	Sim.	Obs.	Sim.	Obs.	Sim.	Obs.	Sim.	Obs.	Sim.
1^{st} moment	6.370	7.017	227.525	238.680	17.925	18.807	6.961	7.445	17.472	18.869
2^{nd} moment	2.657	2.867	131.281	143.096	1.692	1.572	1.016	0.935	4.035	3.712
3^{rd} moment	0.639	0.565	40.347	43.666	0.030	0.054	0.051	0.043	0.023	0.025
4^{th} moment	0.272	0.243	10.219	11.036	0.068	0.073	0.028	0.029	0.176	0.195

to $\pm 15\%$, which is acceptable in our planning application. However, more accurate estimation from the stochastic variables realizes a more accurate result. Furthermore, the dependence structure of the stochastic variables are analyzed through the climocagram, as shown in Figure 8. To account for the double periodicity (diurnal and seasonal) of the stochastic variables [72], we also show the daily scale and annual scale, which causes changes in the climocagram, as shown in Figure 8. Also, we show a 8760 days window of the observed data vs. simulated data, where some deviations can be observed between the simulated data and observed.

One of the main features of the hydrometeorological processes (such as wind speed [73] and solar irradiance [74]) is the double periodicity, interpreting the diurnal and seasonal variation of these uncertain variables. Note that the seasonality occurs considering the deterministic movement of the earth in orbit around the sun and around its axis of rotation [74]. Hence, we represent the double periodicity of the solar irradiance

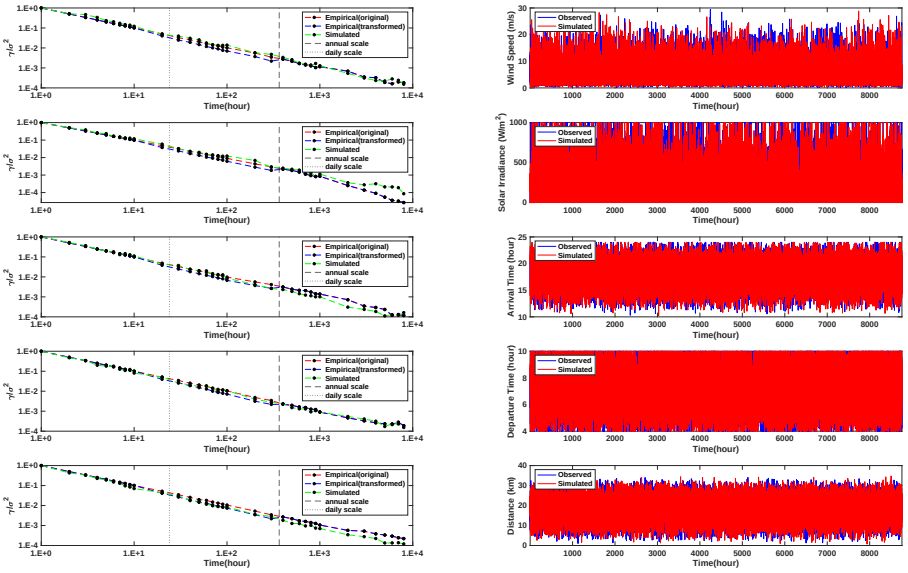

Figure 7: Uncertainty analysis results of stochastic variables, including wind speed, solar irradiance, arrival time of EV, departure time of EV, and distance: [left] climacograms for the empirical and simulated data; [right] a 8760 days window of the observed data vs. simulated data.

and wind speed in Figure 8. It is worthwhile to mention that it is expected to see a double periodicity for the EV stochastic parameters (arrival time, departure time, and traveled distance); however, it is beyond of our study and should be addressed in future works.

There exist several methods to improve the estimation from the stochastic variables and preserve its marginal structure, which may rely on the sufficient length of time series. Although in practical applications, it is difficult to find sufficiently long data for a specific geographical area. Also, the more accurate estimation for preserving the marginal structure of the stochastic variable can be enabled through producing a synthesis time series using approximating the marginal structure and dependence structure, which is justified as an acceptable approach for modeling the intermittencies. It is shown that for an acceptable estimation from the uncertain variable, a time series with a sufficient length is required (e.g., 10^5 for a Hurst-Kolmogorov process) [75], while our time series has a length of $n = 5 \times 8760$. It has been proposed in [61] to model the intermittencies of the stochastic variables through the extended symmet-

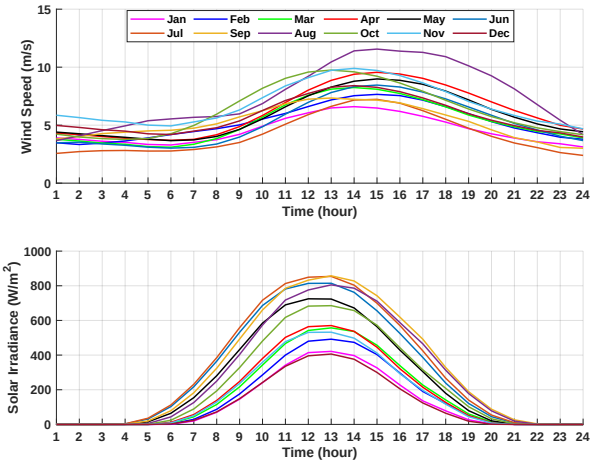

Figure 8: Double periodicity diagram for wind speed (top) and solar irradiance (bottom), interpreting average recorded value for each hour.

ric moving average method, which has been justified to preserve the structure of the stochastic variables. We will aim to apply the extended symmetric moving average method presented by [76], which seems very efficient and more practical, to model the uncertainties and produce the estimated data in future work and justify the obtained results with the estimated data through the machine learning algorithm.

7.2.2. Simulation results of the proposed method

To visualize the performance of the proposed method, the voltages of the MMG nodes are presented in Figure 9, describing the voltage range of each node over a one-year period. Hence, the voltage stability goal, i.e., keeping the voltage profile at each node within the safe limits of 0.95 to 1.05 pu, is met. The voltage results verify finding the optimal solution for our stochastic planning algorithm that satisfies the operational constraints, e.g., voltage limits. Furthermore, keeping the voltage under 1.05 pu decreases the power losses and extra cost for electricity production to supply the demand.

The primary MCP should be determined to advance the power transactions in the electricity market, which is thoroughly discussed in Section 2. To determine the primary MCP, the DNO receives the power bids from the MMG. Afterward, the power

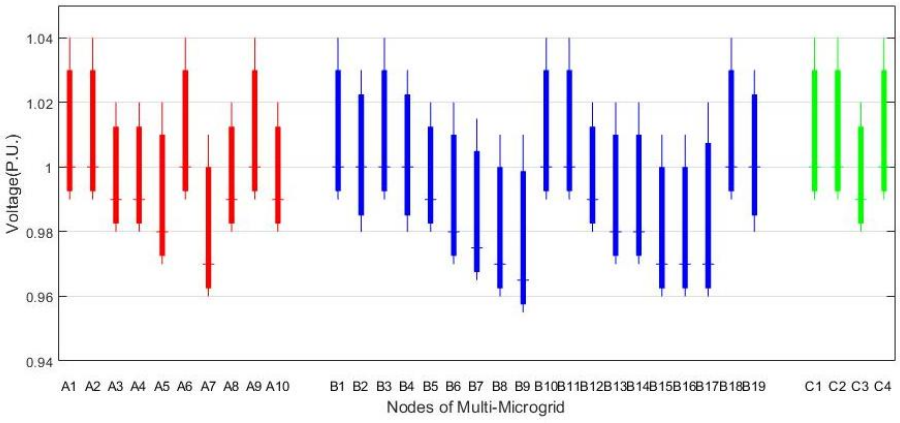

Figure 9: Voltages of the multi-microgrid nodes.

bids and the prices are sorted, and the primary MCP is found. The electricity price of the DNO, the primary MCP, and the final MCP are illustrated in Figure 10. As observed in this figure, the final MCP interprets the dynamic real-time electricity market, providing competitive trading circumstances. Hence, the RER-based MMG can participate in the real-time electricity market and compete with fossil fuel-based resources.

Furthermore, the optimal cost and size of RERs and ES in the MMG are represented in Figure 11. The main objective of the proposed stochastic planning algorithm is to minimize the MMG's cost, which impacts all the MGs' cost. The optimal costs obtained through the stochastic planning algorithm are justified with considering no interactions with the electricity market, where the decreasing cost verifies the importance of modeling interactions between the MMG and the electricity market. The cost reduction due to MMG participation in the electricity market as the price maker occurs for MGs, but the cost reductions are not the same for all MGs. As discussed earlier, due to the high cost of the FC compared to other resources, the MG1 experiences less cost reduction than other MGs. Moreover, the optimal size of RERs and ES are determined by the proposed methodology and compared with the case of considering no interactions with the electricity market, showing the size reduction in all resources considering the interactions between the MMG and electricity market. All the RERs and ES face the size reduction after the MMG participation in the electricity market. Comparing the

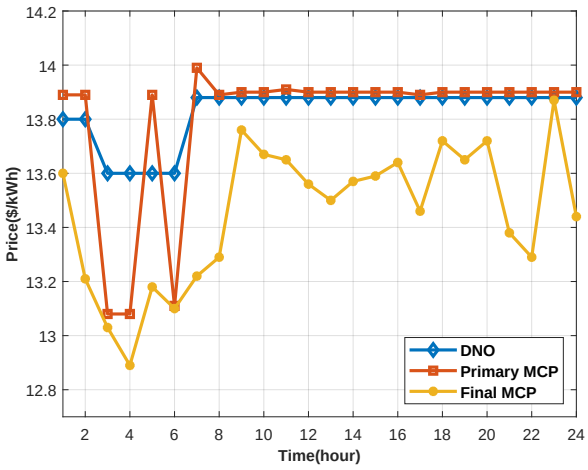

Figure 10: Electricity price in the real-time electricity market.

MMG participation as a price maker in the electricity market to the case of MMG as a price taker highlights the better performance of the proposed method.

Finally, to validate the efficiency of the QPSO algorithm to solve the optimization problem (i.e., cost minimization in our problem), the obtained results are compared with two heuristic optimization algorithms of genetics algorithm (GA), as well as particle swarm optimization (PSO) method. Hence, the optimization algorithm is solved through the GA and PSO methods, where the QPSO algorithm shows better accuracy and convergence speed than other algorithms. The total costs of MMG considering no interactions with the electricity market, optimization enabled through the GA, optimization enabled through the PSO, and optimization enabled through the QPSO are 457.694 million $, 429.737 million $, 424.537 million $, and 416.850 million $, respectively. Furthermore, the QPSO transcends other methods in convergence speed due to its powerful search in response space.

7.3. Discussions

In this study, we present a stochastic planning algorithm, which investigates the performance of the MMG as a price maker and the corresponding effects on the MMG's operation and cost. In this regard, our study differs from the previous studies, assuming the MMG as a price taker, where a significant role of this approach in decreasing the

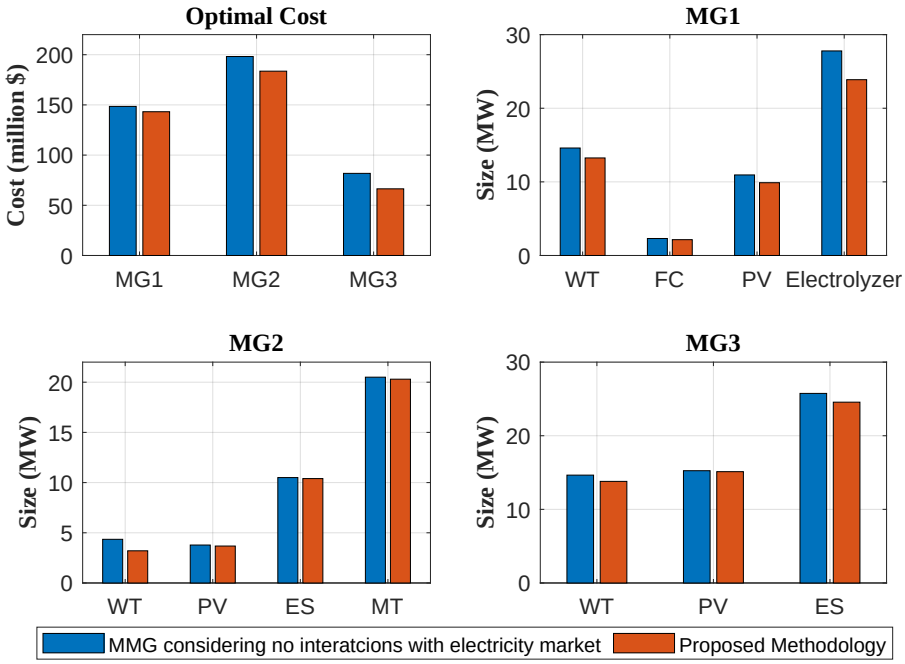

Figure 11: Optimal cost and size for a multi-microgrid considering no interactions with electricity market vs. proposed methodology, assuming the multi-microgrid as a price maker in the electricity market.

total cost of the MMG, as well as the reduced size of the RERs are verified. Due to the increased integration of the uncertain resources to the MG, we perform a detailed uncertainty analysis by comparing the simulated (i.e., estimated) data along with the observed data. Specifically, we focus on the five stochastic variables, including wind speed, solar irradiance, arrival time of EV, departure time of EV, and distance in this study, where we show the stochastic variable structure in terms of marginal structure and second-order dependence structure. Although our method for modeling the uncertainties in the stochastic variable is accurate enough for our application, better accuracy may be achieved through the stochastic methods to estimate the synthesis time series [61], which will be investigated in future studies. It should be noted that the stochastic planning of the MMG improves the reliability of the future MMG. The proposed approach analyzes the MMG role as the price maker in the electricity market to pave a way towards the increased RER-based MMG; however, the MMG is considered a price

taker in the current structure.

8. Conclusions

We presented a stochastic planning algorithm for an MMG considering the high penetration of RERs and participation of the MMG as the price maker in the real-time electricity market. The dynamic behavior of the real-time electricity market and the uncertain parameters were thoroughly modeled, enabling the algorithm to hedge against intermittencies that may increase the total cost and followed with an unreliable grid. A cost minimization problem was formulated to model the stochastic planning optimization algorithm due to the operational constraints. The presented methodology was verified through a sample MMG, where its superiority was shown compared to the case of considering no interactions with the electricity market. A detailed uncertainty analysis was presented in our paper, where we considered the Copula method to correct the error arisen due to the prediction based on the observed data. The obtained results verified an average 8% cost reduction in the MMG due to the active participation in the real-time electricity market.

Future work will focus on the dynamic analysis and shifting to a minute basis due to the sudden changes in load and generation that happen on a minute by minute basis, which was not considered in our study. Also, one of the major problems in developing the price maker MMG is their size and corresponding effects on the electricity market, which will be thoroughly analyzed in future works. On the other hand, the uncertainty analysis should be thoroughly expanded in future work to justify various approaches in estimating the uncertain variable while preserving the stochastic structure. One of the main research gaps is to analyze the double periodicity of the EV stochastic variables, which should be addressed through detailed analysis of sufficient recorded data for EV. Finally, it is of interest to extend the proposed methodology to the energy market, assuming the thermal loads and resources, as well as electrical resources.

References

[1] Z. Abdmouleh, A. Gastli, L. Ben-Brahim, M. Haouari, N. A. Al-Emadi, Review of optimization techniques applied for the integration of distributed generation from renewable energy sources, Renewable Energy 113 (2017) 266–280.

[2] A. Jafari, H. G. Ganjehlou, T. Khalili, A. Bidram, A fair electricity market strategy for energy management and reliability enhancement of islanded multi-microgrids, Applied Energy 270 (2020) 115170.

[3] A. Hasankhani, S. M. Hakimi, Stochastic energy management of smart microgrid with intermittent renewable energy resources in electricity market, Energy 219 (2021) 119668.

[4] C. S. Lai, M. D. McCulloch, Sizing of stand-alone solar pv and storage system with anaerobic digestion biogas power plants, IEEE Transactions on Industrial Electronics 64 (3) (2016) 2112–2121.

[5] M. Åberg, D. Lingfors, J. Olauson, J. Widén, Can electricity market prices control power-to-heat production for peak shaving of renewable power generation? the case of sweden, Energy 176 (2019) 1–14.

[6] J. Faraji, A. Abazari, M. Babaei, S. Muyeen, M. Benbouzid, Day-ahead optimization of prosumer considering battery depreciation and weather prediction for renewable energy sources, Applied Sciences 10 (8) (2020) 2774.

[7] P. Li, R.-X. Li, Y. Cao, D.-Y. Li, G. Xie, Multiobjective sizing optimization for island microgrids using a triangular aggregation model and the levy-harmony algorithm, IEEE Transactions on Industrial Informatics 14 (8) (2017) 3495–3505.

[8] J. Faraji, M. Babaei, N. Bayati, M. A Hejazi, A comparative study between traditional backup generator systems and renewable energy based microgrids for power resilience enhancement of a local clinic, Electronics 8 (12) (2019) 1485.

[9] C. Wouters, E. S. Fraga, A. M. James, An energy integrated, multi-microgrid, milp (mixed-integer linear programming) approach for residential distributed energy system planning–a south australian case-study, Energy 85 (2015) 30–44.

[10] D. Wang, X. Guan, J. Wu, P. Li, P. Zan, H. Xu, Integrated energy exchange scheduling for multimicrogrid system with electric vehicles, IEEE Transactions on Smart Grid 7 (4) (2015) 1762–1774.

[11] Y. Du, F. Li, Intelligent multi-microgrid energy management based on deep neural network and model-free reinforcement learning, IEEE Transactions on Smart Grid 11 (2) (2019) 1066–1076.

[12] S. E. Ahmadi, N. Rezaei, A new isolated renewable based multi microgrid optimal energy management system considering uncertainty and demand response, International Journal of Electrical Power & Energy Systems 118 (2020) 105760.

[13] N. Bazmohammadi, A. Tahsiri, A. Anvari-Moghaddam, J. M. Guerrero, Stochastic predictive control of multi-microgrid systems, IEEE Transactions on Industry Applications 55 (5) (2019) 5311–5319.

[14] H. Qiu, F. You, Decentralized-distributed robust electric power scheduling for multi-microgrid systems, Applied Energy 269 (2020) 115146.

[15] J. Faraji, A. Ketabi, H. Hashemi-Dezaki, M. Shafie-Khah, J. P. Catalão, Optimal day-ahead scheduling and operation of the prosumer by considering corrective actions based on very short-term load forecasting, IEEE Access 8 (2020) 83561–83582.

[16] J. Faraji, A. Ketabi, H. Hashemi-Dezaki, M. Shafiekhah, J. P. Catalão, Optimal day-ahead self-scheduling and operation of prosumer microgrids using hybrid machine learning-based weather and load forecasting, IEEE Access.

[17] F. H. Aghdam, N. T. Kalantari, B. Mohammadi-Ivatloo, A stochastic optimal scheduling of multi-microgrid systems considering emissions: A chance constrained model, Journal of Cleaner Production 275 (2020) 122965.

[18] X. Mo, J. Zhu, J. Chen, Y. Guo, Y. Xia, M. Liu, A stochastic spatiotemporal decomposition decision-making approach for real-time dynamic energy management of multi-microgrids, IEEE Transactions on Sustainable Energy.

[19] L. Xiong, P. Li, Z. Wang, J. Wang, Multi-agent based multi objective renewable energy management for diversified community power consumers, Applied energy 259 (2020) 114140.

[20] Z. Liu, J. Gao, H. Yu, X. Wang, Operation mechanism and strategies for transactive electricity market with multi-microgrid in grid-connected mode, IEEE Access 8 (2020) 79594–79603.

[21] A. D. Tesfamicael, V. Liu, M. Mckague, W. Caelli, E. Foo, A design for a secure energy market trading system in a national wholesale electricity market, IEEE Access 8 (2020) 132424–132445.

[22] J. An, M. Lee, S. Yeom, T. Hong, Determining the peer-to-peer electricity trading price and strategy for energy prosumers and consumers within a microgrid, Applied Energy 261 (2020) 114335.

[23] H. Golmohamadi, A. Asadi, A multi-stage stochastic energy management of responsive irrigation pumps in dynamic electricity markets, Applied Energy 265 (2020) 114804.

[24] Y. Zhou, W. Yu, S. Zhu, B. Yang, J. He, Distributionally robust chance-constrained energy management of an integrated retailer in the multi-energy market, Applied Energy 286 (2021) 116516.

[25] H. Haghighat, H. Karimianfard, B. Zeng, Integrating energy management of autonomous smart grids in electricity market operation, IEEE Transactions on Smart Grid 11 (5) (2020) 4044–4055.

[26] U. Akram, M. Khalid, S. Shafiq, Optimal sizing of a wind/solar/battery hybrid grid-connected microgrid system, IET Renewable Power Generation 12 (1) (2017) 72–80.

[27] P. Firouzmakan, R.-A. Hooshmand, M. Bornapour, A. Khodabakhshian, A comprehensive stochastic energy management system of micro-chp units, renewable energy sources and storage systems in microgrids considering demand response programs, Renewable and Sustainable Energy Reviews 108 (2019) 355–368.

[28] M. Dabbaghjamanesh, S. Mehraeen, A. Kavousi-Fard, F. Ferdowsi, A new efficient stochastic energy management technique for interconnected ac microgrids, in: 2018 IEEE Power & Energy Society General Meeting (PESGM), IEEE, 2018, pp. 1–5.

[29] P. Kou, D. Liang, L. Gao, Distributed empc of multiple microgrids for coordinated stochastic energy management, Applied energy 185 (2017) 939–952.

[30] A. S. Farsangi, S. Hadayeghparast, M. Mehdinejad, H. Shayanfar, A novel stochastic energy management of a microgrid with various types of distributed energy resources in presence of demand response programs, Energy 160 (2018) 257–274.

[31] S. Nojavan, K. Zare, B. Mohammadi-Ivatloo, Optimal stochastic energy management of retailer based on selling price determination under smart grid environment in the presence of demand response program, Applied energy 187 (2017) 449–464.

[32] F. Sheidaei, A. Ahmarinejad, Multi-stage stochastic framework for energy management of virtual power plants considering electric vehicles and demand response programs, International Journal of Electrical Power & Energy Systems 120 (2020) 106047.

[33] S. M. Nosratabadi, R.-A. Hooshmand, Stochastic electrical energy management of industrial virtual power plant considering time-based and incentive-based demand response programs option in contingency condition, International Journal of Emerging Electric Power Systems 1 (ahead-of-print).

[34] J. Chen, F. Wang, K. A. Stelson, A mathematical approach to minimizing the cost of energy for large utility wind turbines, Applied energy 228 (2018) 1413–1422.

[35] S. Abapour, B. Mohammadi-Ivatloo, M. T. Hagh, Robust bidding strategy for demand response aggregators in electricity market based on game theory, Journal of Cleaner Production 243 (2020) 118393.

[36] W. Amin, Q. Huang, M. Afzal, A. A. Khan, K. Umer, S. A. Ahmed, A converging non-cooperative & cooperative game theory approach for stabilizing peer-to-peer electricity trading, Electric Power Systems Research 183 (2020) 106278.

[37] Y. Jiang, K. Zhou, X. Lu, S. Yang, Electricity trading pricing among prosumers with game theory-based model in energy blockchain environment, Applied Energy 271 (2020) 115239.

[38] M. Pied, M. F.Anjos, R. P.Malhame, A flexibility product for electric water heater aggregators on electricity markets, Applied Energy 280 (2020) 115168.

[39] H. Khaloie, M. Mollahassani-pour, A. Anvari-Moghaddam, Optimal behavior of a hybrid power producer in day-ahead and intraday markets: A bi-objective cvar-based approach, IEEE Transactions on Sustainable Energy.

[40] Q. Chen, P. Zou, C. Wu, J. Zhang, M. Li, Q. Xia, C. Kang, A nash-cournot approach to assessing flexible ramping products, Applied Energy 206 (2017) 42–50.

[41] M. Motalleb, P. Siano, R. Ghorbani, Networked stackelberg competition in a demand response market, Applied Energy 239 (2019) 680–691.

[42] F. S. Oliveira, C. Ruiz, Analysis of futures and spot electricity markets under risk aversion, European Journal of Operational Research.

[43] S. M. Hakimi, H. Bagheritabar, A. Hasankhani, M. Shafie-khah, M. Lotfi, J. P. Catalão, Planning of smart microgrids with high renewable penetration considering electricity market conditions, in: 2019 IEEE International Conference on Environment and Electrical Engineering and 2019 IEEE Industrial and Commercial Power Systems Europe (EEEIC/I&CPS Europe), IEEE, 2019, pp. 1–5.

[44] S. M. Hakimi, A. Hasankhani, M. Shafie-Khah, J. P. Catalão, Demand response method for smart microgrids considering high renewable energies penetration, Sustainable Energy, Grids and Networks (2020) 100325.

[45] L. Gubler, G. G. Scherer, Trends for fuel cell membrane development, Desalination 250 (3) (2010) 1034–1037.

[46] [link].
URL https://www.energy.gov

[47] E. Shahrabi, S. M. Hakimi, A. Hasankhani, G. Derakhshan, B. Abdi, Developing optimal energy management of energy hub in the presence of stochastic renewable energy resources, Sustainable Energy, Grids and Networks 26 (2021) 100428.

[48] F. Ramadhani, M. A. Hussain, H. Mokhlis, M. Fazly, J. M. Ali, Evaluation of solid oxide fuel cell based polygeneration system in residential areas integrating with electric charging and hydrogen fueling stations for vehicles, Applied Energy 238 (2019) 1373–1388.

[49] X. Gong, F. Dong, M. A. Mohamed, O. M. Abdalla, Z. M. Ali, A secured energy management architecture for smart hybrid microgrids considering pem-fuel cell and electric vehicles, IEEE Access 8 (2020) 47807–47823.

[50] H. Khaloie, A. Anvari-Moghaddam, N. Hatziargyriou, J. Contreras, Risk-constrained self-scheduling of a hybrid power plant considering interval-based intraday demand response exchange market prices, Journal of Cleaner Production 282 (2021) 125344.

[51] M. Nizami, A. Haque, P. Nguyen, M. Hossain, On the application of home energy management systems for power grid support, Energy 188 (2019) 116104.

[52] A. Hasankhani, S. M. Hakimi, Optimal charge scheduling of electric vehicles in smart homes, in: Electric Vehicles in Energy Systems, Springer, 2020, pp. 359–383.

[53] Renewable energy and energy efficiency organization (satba).
URL http://www.satba.gov.ir

[54] M. Mehrjoo, M. J. Jozani, M. Pawlak, Wind turbine power curve modeling for reliable power prediction using monotonic regression, Renewable Energy 147 (2020) 214–222.

[55] E. Pashajavid, M. A. Golkar, Charging of plug-in electric vehicles: Stochastic modelling of load demand within domestic grids, in: 20th Iranian Conference on Electrical Engineering (ICEE2012), IEEE, 2012, pp. 535–539.

[56] E. Shahryari, H. Shayeghi, B. Mohammadi-Ivatloo, M. Moradzadeh, A copula-based method to consider uncertainties for multi-objective energy management of microgrid in presence of demand response, Energy 175 (2019) 879–890.

[57] H. V. Haghi, M. T. Bina, M. Golkar, S. Moghaddas-Tafreshi, Using copulas for analysis of large datasets in renewable distributed generation: Pv and wind power integration in iran, Renewable Energy 35 (9) (2010) 1991–2000.

[58] S. Hagspiel, A. Papaemannouil, M. Schmid, G. Andersson, Copula-based modeling of stochastic wind power in europe and implications for the swiss power grid, Applied energy 96 (2012) 33–44.

[59] F. Ielpo, C. Merhy, G. Simon, Engineering Investment Process: Making Value Creation Repeatable, Elsevier, 2017.

[60] W. P. J. Philippe, S. Zhang, S. Eftekharnejad, P. K. Ghosh, P. K. Varshney, Mixed copula-based uncertainty modeling of hourly wind farm production for power system operational planning studies, IEEE Access 8 (2020) 138569–138583.

[61] P. Dimitriadis, D. Koutsoyiannis, Stochastic synthesis approximating any process dependence and distribution, Stochastic environmental research and risk assessment 32 (6) (2018) 1493–1515.

[62] P. Dimitriadis, D. Koutsoyiannis, Climacogram versus autocovariance and power spectrum in stochastic modelling for markovian and hurst–kolmogorov processes, Stochastic environmental research and risk assessment 29 (6) (2015) 1649–1669.

[63] S. M. Hakimi, A. Hasankhani, M. Shafie-khah, J. P. Catalão, Optimal sizing and siting of smart microgrid components under high renewables penetration considering demand response, IET Renewable Power Generation 13 (10) (2019) 1809–1822.

[64] Iran grid management company.
URL https://www.igmc.ir/en

[65] V. P. Gountis, A. G. Bakirtzis, Efficient determination of cournot equilibria in electricity markets, IEEE Transactions on Power Systems 19 (4) (2004) 1837–1844.

[66] R. Bahmani, H. Karimi, S. Jadid, Stochastic electricity market model in networked microgrids considering demand response programs and renewable energy sources, International Journal of Electrical Power & Energy Systems 117 (2020) 105606.

[67] [link].
URL https://www.irema.ir

[68] R. Ioannidis, T. Iliopoulou, C. Iliopoulou, L. Katikas, A. Petsou, M.-E. Merakou, M.-E. Asimomiti, N. Pelekanos, G. Koudouris, P. Dimitriadis, et al., Solar-powered bus route: introducing renewable energy into a university campus transport system, Advances in Geosciences 49 (2019) 215–224.

[69] H. Hashemi-Dezaki, H. Askarian-Abyaneh, H. Haeri-Khiavi, Impacts of direct cyber-power interdependencies on smart grid reliability under various penetration levels of microturbine/wind/solar distributed generations, IET Generation, Transmission & Distribution 10 (4) (2016) 928–937.

[70] N. T. Nguyen, R. Matsuhashi, T. T. B. C. Vo, A design on sustainable hybrid energy systems by multi-objective optimization for aquaculture industry, Renewable Energy 163 (2021) 1878–1894.

[71] A. W. Danté, K. Agbossou, S. Kelouwani, A. Cardenas, J. Bouchard, Online modeling and identification of plug-in electric vehicles sharing a residential station, International Journal of Electrical Power & Energy Systems 108 (2019) 162–176.

[72] A. Langousis, D. Koutsoyiannis, A stochastic methodology for generation of seasonal time series reproducing overyear scaling behaviour, Journal of Hydrology 322 (1-4) (2006) 138–154.

[73] I. Deligiannis, P. Dimitriadis, O. Daskalou, Y. Dimakos, D. Koutsoyiannis, Global investigation of double periodicity of hourly wind speed for stochastic simulation; application in greece, Energy Procedia 97 (2016) 278–285.

[74] G. Koudouris, P. Dimitriadis, T. Iliopoulou, N. Mamassis, D. Koutsoyiannis, A stochastic model for the hourly solar radiation process for application in renewable resources management, Advances in Geosciences 45 (2018) 139–145.

[75] P. Dimitriadis, D. Koutsoyiannis, The mode of the climacogram estimator for a gaussian hurst-kolmogorov process, Journal of Hydroinformatics 22 (1) (2020) 160–169.

[76] D. Koutsoyiannis, The hurst phenomenon and fractional gaussian noise made easy, Hydrological Sciences Journal 47 (4) (2002) 573–595.